Chemical Science

EDGE ARTICLE

View Article Online
View Journal | View Issue

Cite this: *Chem. Sci.*, 2018, **9**, 770

Target-activated streptavidin–biotin controlled binding probe†

Yung-Peng Wu,‡[a] Chee Ying Chew,‡[a] Tian-Neng Li,[b] Tzu-Hsuan Chung,[a] En-Hao Chang,[a] Chak Hin Lam[a] and Kui-Thong Tan *[a]

Received 13th September 2017
Accepted 16th November 2017

DOI: 10.1039/c7sc04014h

rsc.li/chemical-science

Target-activated chemical probes are important tools in basic biological research and medical diagnosis for monitoring enzyme activities and reactive small molecules. Based on the fluorescence turn-on mechanism, they can be divided into two classes: dye-based fluorescent probes and caged-luciferin. In this paper, we introduce a new type of chemical probe in which the fluorescence turn-on is based on controlled streptavidin–biotin binding. Compared to conventional probes, the streptavidin–biotin controlled binding probe has several advantages, such as minimal background at its "OFF" state, multiple signal amplification steps, and unlimited selection of the optimal dyes for detection. To expand the scope, a new synthetic method was developed, through which a wider range of analyte recognition groups can be easily introduced to construct the binding probe. This probe design was successfully applied to image and study secreted peroxynitrite ($ONOO^-$) at the cell surface of macrophages where information on $ONOO^-$ is difficult to obtain. As the signals are generated upon the binding of streptavidin to the biotin probe, this highly versatile design can not only be used in fluorescence detection but can also be applied in various other detection modes, such as electrochemical and enzyme-amplified luminescence detection.

Introduction

Chemical probes are important tools in basic biological research and medical diagnosis because they allow for sensitive, simple, and specific detection of the target molecules in complex environments, such as cell lysates, living cells, and *in vivo*.[1,2] Currently, most chemical probes are reaction-based and designed for monitoring enzyme activities and reactive small molecules using fluorescence detection technique.[3–5] Based on the fluorescence turn-on mechanism, they can be divided into two classes: dye-based fluorescent probes and caged-luciferin. In the presence of a target molecule, the fluorophore of the fluorescent probe can be turned-on *via* FRET, PET, AIE, or the restoration of fluorophore π-conjugation,[6–9] while the fluorescence turn on mechanism of caged-luciferin is based on the specific enzymatic reaction of luciferase with luciferin to emit yellow to green light.[10]

Although undoubtedly valuable and widely described in the literature, these two chemical probe designs pose several limitations. The first limitation is the presence of intrinsic background fluorescence from the "fluorescence off" probe. Regardless of how efficiently the fluorescence of the dye molecule is suppressed before target activation, the fluorescent probe will always emit a very weak background fluorescence in its "OFF" state. As a result, the analytical sensitivity of the probe is reduced. The second limitation is that a reaction-based chemical probe only reacts with one reactive small molecule to produce a single fluorescence signal. This "one target to one signal" detection mode has limited the sensitivity of most fluorescent probes. Although chemical probes based on self-immolative polymers have been reported to achieve "one target to multiple signals" detection, this approach normally requires long synthetic steps to assemble multiple fluorophores into the chemical probe to achieve significant fluorescence amplification.[11] The third limitation is that fluorescence detection is restricted by the type of fluorophore used to construct the fluorescent probe. For example, a fluorescent probe based on Cy5 dye can only be ideally detected by excitation light of around 640 nm. To date, a chemical probe that allows for the liberal choice of excitation and emission wavelengths for fluorescence detection has yet to be reported.

In this paper, we describe a general approach to overcome the three limitations of conventional chemical probes by developing a streptavidin–biotin controlled binding probe (CBP, Fig. 1). The rationale behind this new CBP concept is based on the fact that biotin has extremely high binding affinity ($K_d = 10^{-14}$ M) with streptavidin, while chemical modification at the N′-1 urea nitrogen of biotin to form caged-biotin can

[a]*Department of Chemistry, National Tsing Hua University, 101 Sec. 2, Kuang Fu Rd, Hsinchu 30013, Taiwan, Republic of China. E-mail: kttan@mx.nthu.edu.tw*

[b]*Institute of Molecular and Cellular Biology, Department of Life Science, National Tsing Hua University, 101 Sec. 2, Kuang Fu Rd, Hsinchu 30013, Taiwan, Republic of China*

† Electronic supplementary information (ESI) available. See DOI: 10.1039/c7sc04014h

‡ These authors contributed equally.

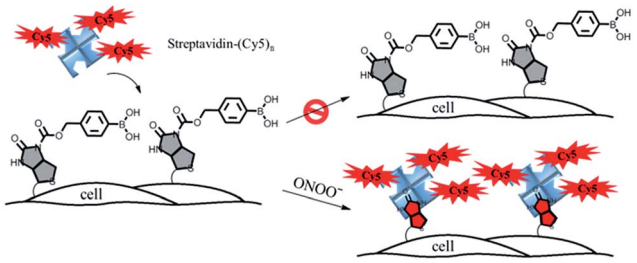

Fig. 1 A schematic illustration of the membrane-anchored streptavidin–biotin controlled binding probe for the imaging of $ONOO^-$ at the cell surface.

dramatically reduce its streptavidin binding affinity ($K_d \approx 10^{-5}$ M).[12] In the absence of the target analyte, the CBP on the cell surface would not be able to bind with fluorophore conjugated streptavidin due to the low binding affinity of caged-biotin with streptavidin. The fluorophore conjugated streptavidin can then be washed away to eliminate any background fluorescence. In the presence of the target analyte triggering biotin uncaging, the fluorophore conjugated streptavidin would bind to the biotin probe. As there are multiple fluorophore units on one streptavidin molecule, significant signal amplification can be achieved. Furthermore, streptavidin conjugated with different bright fluorophores, such as Cy5, Cy3 or Alexa488, can be added on demand to generate the desired fluorescence signals. Thus, detection is no longer restricted by the type of fluorescent dye, such as in the case of fluorescent probes. Since the fluorescence turn-on mechanism is different from the fluorescent probes and caged-luciferin, this novel CBP approach can be considered as a third type of chemical probe. This CBP approach would be very useful for the detection of a low concentration of reactive oxygen and nitrogen species (ROS/RNS), such as H_2O_2, $ONOO^-$, and HOCl. Currently, ROS/RNS are mostly detected by fluorescent probes that react rapidly with the ROS/RNS to produce dramatic changes in the absorption and fluorescence signals.[13–16]

The CBP approach was applied to image and study local peroxynitrite ($ONOO^-$) secreted from the plasma membrane of macrophages upon phorbol-12-myristate-13-acetate (PMA) stimulation.[17,18] $ONOO^-$ is a RNS and plays multiple roles in biological processes. It may exert a contributory effect by participating in microorganism killing and nitrosylation signaling.[19,20] It can also be deleterious due to its nitrosative damage to lipids, proteins, and DNA. Therefore, $ONOO^-$ is widely assumed to account for most of the cytotoxicity previously ascribed to NO and O_2^-. Although several fluorescent probes have been described previously for the detection of $ONOO^-$, all of them either detect $ONOO^-$ in the bulk solution or in cytosol, but not $ONOO^-$ secretion along the plasma membrane.[21–25] The difficulty in detecting local $ONOO^-$ immediately after its secretion from the extracellular surface can be attributed to two main reasons: the fast diffusion of $ONOO^-$ to the bulk solution and the limited sensitivity of the existing chemical probes to detect very low concentrations of $ONOO^-$ at the cell surface. We believe that the ability to detect and image local $ONOO^-$ along the extracellular surface of a single cell is biologically significant as the plasma membrane is where most of the ROS and RNS exert their functions for host defense and signal transductions.

In order to image membrane secreted $ONOO^-$ in the living cells, we constructed a cell-impermeable membrane-anchored streptavidin–biotin controlled binding probe, **ONOO-CBP**, which contains an $ONOO^-$ responsive boronic acid moiety and a sulfo-NHS ester moiety (Scheme 1). **ONOO-CBP** can be anchored onto the cell surface *via* the reaction of the sulfo-NHS moiety with the amine of the cell membrane proteins and the boronic acid group is hence well-placed to react with the secreted $ONOO^-$ to form phenol, which concomitantly triggers the cleavage of the carbamate group to activate the probe for binding with the streptavidin–fluorophore (Fig. S1†). While the boronate derivatives were first described to detect H_2O_2,[26,27] it was determined recently that boronate reacts stoichiometrically and rapidly with $ONOO^-$ ($k = 1.1 \times 10^6\ M^{-1}\ s^{-1}$) in comparison to the slower reaction rate with H_2O_2 ($k \sim 1\ M^{-1}\ s^{-1}$).[23] Thus, the fast reaction between boronate and $ONOO^-$ should enable the membrane-anchored **ONOO-CBP** probe to capture the secreted $ONOO^-$ at the extracellular membrane before its degradation and/or diffusion into the bulk solution.

Results and discussion

Synthesis of the peroxynitrite-responsive streptavidin–biotin controlled binding probe ONOO-CBP

Although it has been well known that chemical modification at the N′-1 urea nitrogen of biotin can dramatically reduce its binding affinity with streptavidin, all the caged-biotins previously reported were mainly applied to protein site-specific immobilization to retain the protein activities by photo- or electrochemical stimulation.[12,28–30] To date, the caged-biotin approach has yet to be applied directly for analyte detection. The main reason is that caged-biotin with chemical modification at the N′-1 urea nitrogen is difficult to prepare due to the

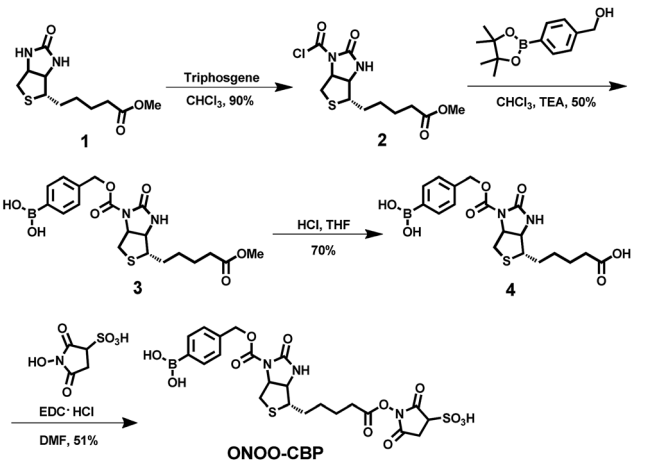

Scheme 1 The synthesis of the cell-impermeable membrane-anchored streptavidin–biotin controlled binding probe, **ONOO-CBP**, for the detection of secreted $ONOO^-$ at the extracellular surface.

low reactivity of the N′-1 urea nitrogen. Therefore, only the highly reactive acyl chloride moiety can be used as an electrophile, which limits the types of chemical modification that can be introduced on the N′-1 urea nitrogen.

In order to develop this CBP strategy as a general design, we developed a new synthetic method to prepare caged-biotin derivatives, through which a wider range of chemical modifications can be easily introduced on the N′-1 urea nitrogen of biotin (Scheme 1). The synthesis commences with the reaction of triphosgene with methyl ester biotin to form the important biotin derivative **2**, which can then be reacted with different types of nucleophile to form the caged-biotin derivatives. It is important to note that compound **2** is stable enough to be purified by column chromatography, which greatly enhances its practicability. Following the acid hydrolysis of the methyl ester, compound **3** was reacted with sulfo-NHS under standard ester coupling conditions to generate the target product, **ONOO-CBP**. When stored in an acidic medium at −80 °C, **ONOO-CBP** was stable for at least two months without signs of degradation (Fig. S2†). This synthetic method is highly versatile as nucleophiles containing different analyte-responsive groups, such as nitro, TBDPS, and TPA, can be reacted with compound **2** to obtain different caged-biotin derivatives (Scheme S2†). Previously, these three moieties have been used for the detection of nitroreductase and fluoride and Cu(I) ions.[31–33]

Imaging of exogenous $ONOO^-$ and selectivity studies

To establish the applicability of **ONOO-CBP** to image secreted $ONOO^-$ at the cell surface, we first employed 3-morpholinosydnonimine hydrochloride (SIN-1) as an external source of $ONOO^-$ to characterize **ONOO-CBP**.[34,35] In a buffer or biological medium, SIN-1 can slowly release NO and O_2^-, which can then combine to form $ONOO^-$. Using the existing method, we have determined that 100 μM SIN-1 can generate about 7% of $ONOO^-$ in one hour (Fig. S3†).[36,37] We labeled the cell surface of the RAW264.7 macrophages with 10 μM **ONOO-CBP** in HBSS buffer for 30 minutes at 37 °C. The unreacted **ONOO-CBP** was removed by washing with the medium, followed by the treatment of 100 μM SIN-1 for 60 minutes at 37 °C to uncage the biotin probe. After the removal of excess SIN-1, streptavidin–Cy5 was added and incubated for 10 minutes. Fluorescent images were taken immediately after the excess unbound streptavidin–Cy5 was washed away. For the cells treated with SIN-1, strong fluorescence was only observed along the plasma membrane of the RAW264.7 cells, while minimal fluorescence was detected in the absence of SIN-1 (Fig. 2a and S4†). When SIN-1 was incubated with 250 μM 4-(hydroxymethyl)phenylboronic acid (BA) for 60 minutes, the fluorescence was reduced dramatically, indicating that the strong fluorescence observed on the cell surface is due to the specific reaction of $ONOO^-$ with the boronic acid moiety of **ONOO-CBP** (Fig. 2aiii). Notably, the fluorescence was barely detectable inside the cells, indicating the practicability of our CBP approach to image secreted $ONOO^-$ along the plasma membrane. This is because the large streptavidin–Cy5 cannot diffuse easily across the plasma membrane to cause nonspecific fluorescence inside the cells.

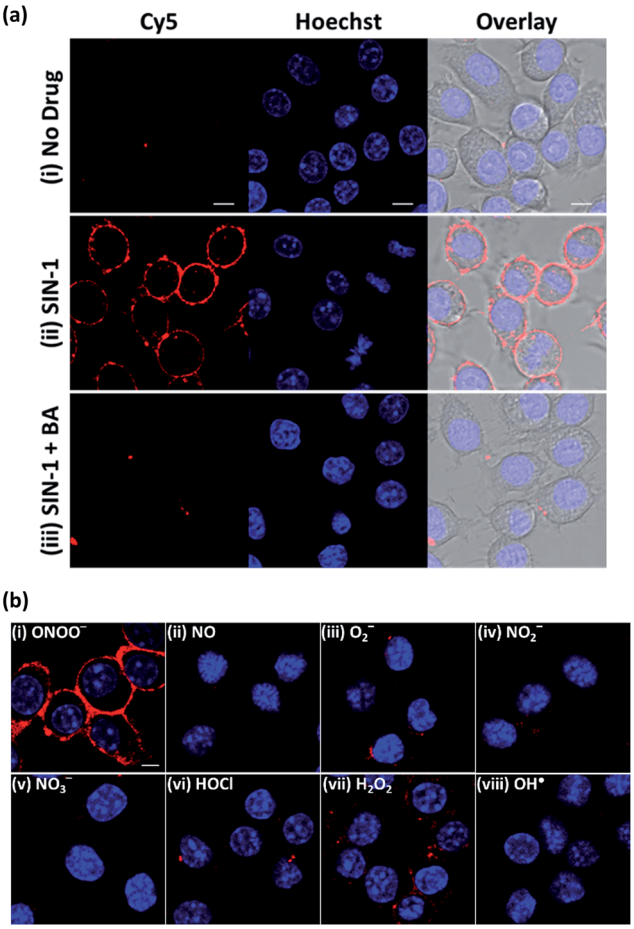

Fig. 2 The fluorescence response of the **ONOO-CBP** labeled RAW264.7 cells after incubation with different exogenous ROS and RNS for 60 minutes. (a) The live cell imaging of the **ONOO-CBP** labeled RAW264.7 cells in (i) the absence or (ii) the presence of 100 μM SIN-1 or (iii) 250 μM BA with 100 μM SIN-1. (b) The live cell imaging of the **ONOO-CBP** labeled RAW264.7 cells in the presence of (i) 50 μM SIN-1 or 100 μM each of (ii) NO, (iii) O_2^-, (iv) NO_2^-, (v) NO_3^-, (vi) HOCl, (vii) H_2O_2, or (viii) $OH^•$. The cell surface stained with streptavidin–Cy5 is shown in red and the nuclei labeled with Hoechst 34580 are shown in blue. Scale bar: 20 μm.

Furthermore, the specific and bright fluorescence on the plasma membrane of the macrophages indicates that the immobilization of **ONOO-CBP** on the cell surface using NHS ester chemistry is an effective approach to generate high quality images. The cytotoxicity test using MTT assays indicates that the labeling of the extracellular surface with **ONOO-CBP** was not cytotoxic for the cells (Fig. S5†).

To further evaluate the applicability of **ONOO-CBP** for imaging $ONOO^-$ on the extracellular membrane, we proceeded to perform several selectivity tests with other ROS and RNS. As shown in Fig. 2b, bright fluorescence was obtained only in the presence of SIN-1, while the treatment of the cells with H_2O_2, $OH^•$, O_2^-, NO, HOCl, NO_2^-, and NO_3^- gave either weak or no detectable fluorescence along the membrane (Fig. S6†).

To validate the controlled binding probe concept *in vitro*, we have also synthesized a fluorogenic caged biotin probe **ONOO-**

SBD, which can be activated by $ONOO^-$ for binding with avidin (a streptavidin derivative with equal biotin affinity) to generate strong fluorescence (Fig. S7 and Scheme S3†).[31] **ONOO-SBD** consists of an environment-sensitive dye, SBD, linked with compound **4**. In the absence of $ONOO^-$ or avidin, the probe shows a weak fluorescence signal. Whereas, in the presence of $ONOO^-$, the caged-biotin moiety of the probe can be activated for binding with avidin to produce strong fluorescence. Similar to the imaging results obtained using **ONOO-CBP**, the fluorogenic **ONOO-SBD** probe responded selectively to $ONOO^-$ and the fluorescence increased over time (Fig. S8†).

The streptavidin–biotin controlled binding probe enables fluorescence imaging with diverse excitation and emission light

Besides the high selectivity, there are two additional advantages of this CBP approach for $ONOO^-$ imaging. First, there is no restriction on the fluorescent dye to be used for generating the fluorescent image so long as the dye can be conjugated to streptavidin. In our study, we demonstrated that bright fluorescence can also be generated with streptavidin–Cy3 and streptavidin–Alexa488 (Fig. 3). This feature allows for the use of many previously untapped bright near-infrared dyes for detection. The second advantage is that our CBP approach can achieve further signal amplification due to the fact that one streptavidin contains four biotin binding sites. To illustrate the signal amplification, a cell-impermeable Cy5–biotin was added to the cells that were already stained with streptavidin–Cy3 and streptavidin–Alexa488. After removing the unbound Cy5–biotin, we can observe clear fluorescence along the plasma membrane from the Cy5 channel (Fig. S9†). These two advantages demonstrate the high versatility and promising potential of CBP to detect low concentrations of the ROS and RNS.

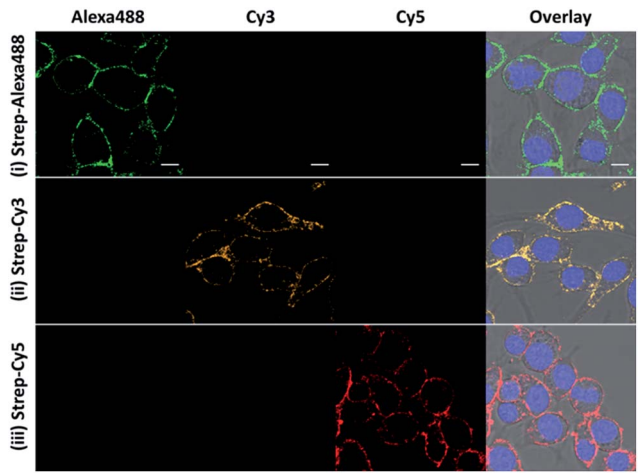

Fig. 3 The fluorescence response of the **ONOO-CBP** labeled RAW264.7 cells after incubation with 100 μM SIN-1 for 60 minutes. After biotin uncaging, the cells were stained with (i) streptavidin–Alexa488, (ii) streptavidin–Cy3, and (iii) streptavidin–Cy5. Scale bar: 20 μm.

Imaging secreted peroxynitrite under PMA stimulation

Next, we focused on assessing the performance of **ONOO-CBP** in imaging endogenously secreted $ONOO^-$ in the RAW264.7 cells, using phorbol-12-myristate-13-acetate (PMA) to stimulate the production of $ONOO^-$. PMA activates phosphokinase C (PKC) to phosphorylate and translocates the NADPH oxidase subunits to the plasma membrane. Upon the assembly of the NADPH oxidase subunits, the membrane-bound NADPH oxidase can produce O_2^-, which can then react with secreted NO to form $ONOO^-$ at diffusion-controlled rates ($k \sim 1 \times 10^{10}$ M^{-1} s^{-1}).[38–40]

To image $ONOO^-$ along the plasma membrane immediately after its secretion, **ONOO-CBP** labeled RAW264.7 macrophages were treated with 1 μg mL^{-1} PMA in DMEM medium for 60 minutes at 37 °C. After staining with streptavidin–Cy5, we observed distinct fluorescence along the extracellular surface of the RAW264.7 cells (Fig. 4a). In the presence of PMA, our membrane-anchored **ONOO-CBP** probe was able to detect that more than 95% of the RAW264.7 cells released $ONOO^-$ (Fig. S10†). On the other hand, no fluorescence was detected in the absence of PMA stimulation. To further demonstrate the quantitative application for detecting secreted $ONOO^-$ in live cells, fluorescence-activated cell sorting (FACS) cytometry was used for the analysis of the RAW264.7 cell population in the

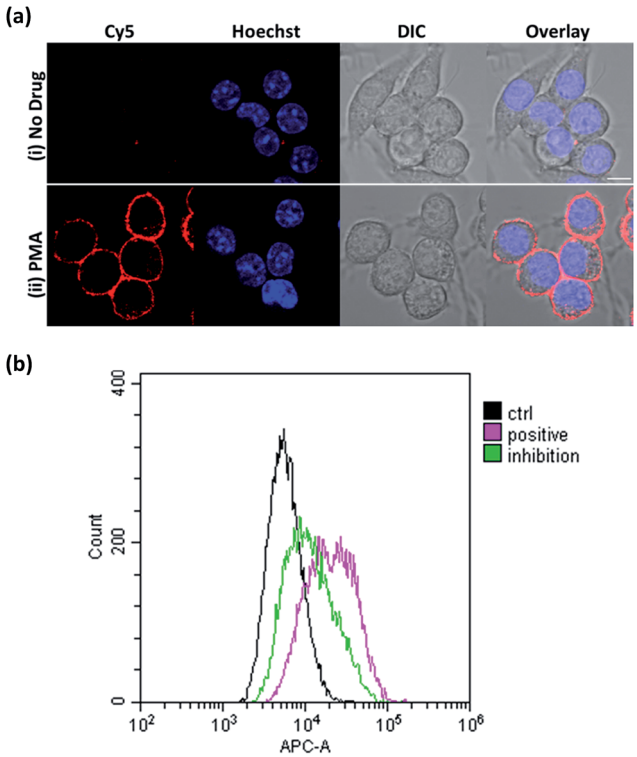

Fig. 4 (a) The live cell imaging of the **ONOO-CBP** labeled RAW264.7 cells in the (i) absence or (ii) presence of 1 μg mL^{-1} PMA after 60 minutes of incubation. Scale bar: 20 μm. (b) The fluorescence-activated cell sorting (FACS) analysis of the **ONOO-CBP** labeled RAW264.7 cells in the absence (black line) or presence (pink line) of 1 μg mL^{-1} PMA after 60 minutes of incubation. The green line indicates the condition in which 15 μg mL^{-1} SOD was mixed with 1 μg mL^{-1} PMA.

absence or presence of PMA. As shown in Fig. 4b, robust streptavidin–Cy5 labeling was observed for the cells treated with PMA, which can be reduced in the presence of superoxide dismutase (SOD) by quenching O_2^-, and this is required in the reaction with NO to form $ONOO^-$. In the absence of PMA, the cells were hardly labeled by streptavidin–Cy5 and showed weaker fluorescence signals. These results showed that membrane-anchored **ONOO-CBP** based on the CBP approach can convincingly detect secreted $ONOO^-$ along the extracellular membrane both at the single cell level and from a population of cells.

The validation of secreted peroxynitrite with various NO, O_2^- and $ONOO^-$ inhibitors

To further validate our membrane-anchored **ONOO-CBP** probe, we examined the fluorescence response of **ONOO-CBP** in the presence of various NO, O_2^- and $ONOO^-$ inhibitors during PMA stimulation. In these experiments, we used 15 μg mL^{-1} superoxide dismustase (SOD) and 1 mM 4-hydroxy-TEMPO (TEMPO) to quench O_2^-, 1 mM N_ω-nitro-L-arginine methyl ester (L-NAME) to suppress NO production by inhibiting NO synthase activity,[41] 1 mM apocynin to inhibit NADPH oxidase,[42,43] 1 mM FeTMPyP, 5 mM uric acid and 250 μM 4-(hydroxymethyl)phenylboronic acid (BA) to quench $ONOO^-$ and 10 μg mL^{-1} catalase separately to show that **ONOO-CBP** would selectively detect $ONOO^-$ and not H_2O_2 during PMA stimulation.

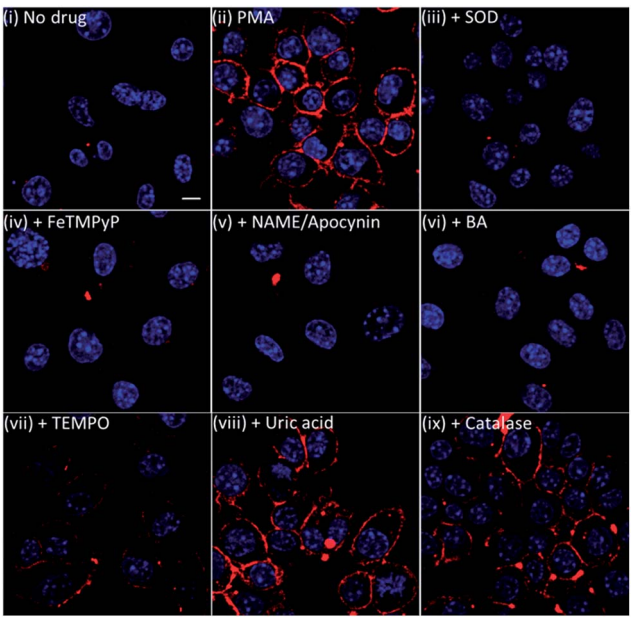

Fig. 5 The live cell imaging of the **ONOO-CBP** labeled RAW264.7 cells in (i) the absence or (ii) the presence of 1 μg mL^{-1} PMA and (iii) PMA + 15 μg mL^{-1} SOD, (iv) PMA + 1 mM FeTMPyP, (v) PMA + 1 mM L-NAME and 1 mM apocynine, (vi) PMA + 250 μM BA, (vii) PMA + 1 mM TEMPO, (viii) PMA + 5 mM uric acid, or (ix) PMA + 10 μg mL^{-1} catalase. Besides the L-NAME/apocynin mixture, which was incubated with the cells for 90 minutes prior to PMA stimulation, all the inhibitors were added to the cells together with PMA and incubated for 60 minutes. The cells were stained with streptavidin–Cy5. Scale bar: 20 μm.

In the presence of SOD, FeTMPyP, L-NAME/apocynin mixture, and BA, we observed minimal fluorescence, similar to the control experiment without PMA treatment (Fig. 5 and S11†). In the presence of TEMPO, weak fluorescence was observed on the cell surface, indicating the partial inhibition of O_2^- to form $ONOO^-$. On the other hand, brighter fluorescence was observed both for the cells treated with uric acid and with catalase. The inability of TEMPO and uric acid to completely quench the endogenous O_2^- and $ONOO^-$ can be attributed to the slower reaction rate of $ONOO^-$ with uric acid ($k = 155\ M^{-1}\ s^{-1}$) and O_2^- with TEMPO ($2.5 \times 10^5\ M^{-1}\ s^{-1}$).[44,45] It was reported that FeTMPyP and boronic acid can react with $ONOO^-$ with very fast reaction rates of $2.2 \times 10^6\ M^{-1}\ s^{-1}$ and $1.1 \times 10^6\ M^{-1}\ s^{-1}$, respectively.[46,47] Furthermore, the reaction rate of O_2^- with SOD is diffusion-limited with a rate of $7 \times 10^9\ M^{-1}\ s^{-1}$.[48] From these kinetic data, we believe that there is a rapid reaction between O_2^- and NO to form $ONOO^-$, which can then react instantly with the membrane-anchored **ONOO-CBP** and lead to the failure of uric acid and TEMPO to completely deplete the $ONOO^-$ and O_2^- precursors. Overall, the results from the inhibitor studies and catalase addition confirmed that the membrane-anchored **ONOO-CBP** probe can accurately image $ONOO^-$ secretion on the extracellular surface upon PMA stimulation of the RAW264.7 macrophages.

The initiation and duration of the peroxynitrite burst in RAW264.7 cells under PMA stimulation

Currently, most analytical methods are developed for the detection of $ONOO^-$ in bulk solutions. Although several microelectrode methods have been reported to be able to determine $ONOO^-$ secretion in the vicinity of the plasma membrane, the lack of high spatial resolution and being limited to studying just a few cells in each experiment have severely restricted their real application.[49,50] To date, obtaining accurate information about the time course of $ONOO^-$ release at the plasma membrane remains a very challenging task. In this regard, we believe that our membrane-anchored **ONOO-CBP** probe would not only be able to image $ONOO^-$ secretion in living cells, but also in more precise spatiotemporal resolution.

To gain insights into the initiation and duration of $ONOO^-$ secretion upon PMA stimulation, **ONOO-CBP** labeled RAW264.7 cells were incubated with 1 μg mL^{-1} PMA for 10, 20, 40, 60 and 80 minutes. The imaging results showed time-dependent fluorescence enhancement along the plasma membrane and distinct fluorescence images were obtained within 20 minutes of PMA stimulation (Fig. 6a and S12†). From the fluorescence time course study, it was estimated that most of the $ONOO^-$ ions were released into the extracellular medium within the 40 to 60 minutes after initiation (Fig. 6b). After the bursting period, the secretion of $ONOO^-$ continued but with a slower releasing rate. These results are consistent with the studies of $ONOO^-$ in bulk solutions.[51] To further validate these imaging results and observations, we performed real-time tracking of the PMA-stimulated macrophages without washing away the streptavidin–Cy5 (Fig. S13†). Although the signal-to-background ratio was reduced due to the presence of unbound streptavidin–Cy5,

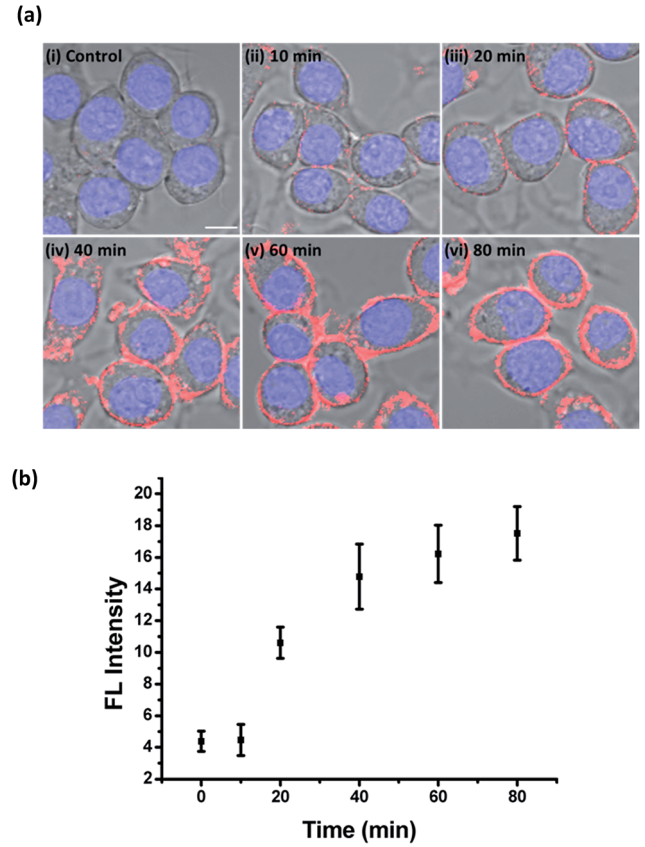

Fig. 6 The time course of $ONOO^-$ secretion into the extracellular medium upon PMA stimulation. (a) The live cell imaging of the **ONOO-CBP** labeled RAW264.7 cells in (i) the absence or presence of 1 μg mL^{-1} PMA after incubation for (ii) 10, (iii) 20, (iv) 40, (v) 60, or (vi) 80 minutes. Scale bar: 20 μm. (b) The time course of the mean fluorescence intensity (processed using Image J) on the cell surface of the RAW264.7 cells treated with 1 μg mL^{-1} PMA ($N = 30$ for each indicated time). The cells were stained with streptavidin–Cy5. Scale bar: 20 μm.

we were still able to track the increase of fluorescence along the plasma membrane over the 110 minute imaging time course.

Conclusion

In conclusion, by controlling the specific interaction of biotin and streptavidin with caged-biotin, we have introduced a new chemical probe design. To expand the scope, a new synthetic method was developed through which a wider range of analyte recognition group can be easily introduced to cage the biotin. The streptavidin–biotin controlled binding probe exhibits significant fluorescence amplification with minimum background and can adopt an unlimited selection of optimal dyes that cannot be achieved by the conventional chemical probes. The application of our controlled binding probe was demonstrated by imaging the $ONOO^-$ secretion at the cell surface of the RAW264.7 macrophages upon PMA stimulation. The $ONOO^-$ secretion from more than 95% of the cells was successfully captured and imaged at the cell surface, and the results were validated by flow cytometry. With this membrane-anchored controlled binding probe, we revealed that the RAW264.7 macrophages secrete $ONOO^-$ within the 20 minutes after PMA treatment and most of the $ONOO^-$ ions have been released into the extracellular medium 40–60 minutes later. Although the application of this CBP approach was demonstrated by imaging secreted $ONOO^-$ at the cell surface in this study, this design can also be used to image analytes inside the cells if a fixed-cell technique is employed (Fig. S14†). As the signals are generated upon the binding of streptavidin to the biotin probe, this highly versatile design can not only be used in fluorescent detection, but it can also be applied in various other detection modes, such as electrochemical and enzyme-amplified luminescence detection.

Conflicts of interest

There are no conflicts to declare.

Acknowledgements

We thank Prof. Lily Hui-Ching Wang for the FACS experiment. We are grateful to the Ministry of Science and Technology (Grant No.: 105-2113-M-007-004) and Ministry of Education ("Aim for the Top University Plan"; Grant No.: 105N501CE1), Taiwan (ROC), for financial support.

Notes and references

1 R. Weissleder, *Nat. Biotechnol.*, 2001, **19**, 316–317.
2 I. Johnson, *The Molecular Probes Handbook: A Guide to Fluorescent Probes and Labeling Technologies*, Life Technologies Corporation, 11th edn, 2010.
3 B. Xing, A. Khanamiryan and J. Rao, *J. Am. Chem. Soc.*, 2005, **127**, 4158–4159.
4 M. Sakabe, D. Asanuma, M. Kamiya, R. J. Iwatate, K. Hanaoka, T. Terai, T. Nagano and Y. Urano, *J. Am. Chem. Soc.*, 2012, **135**, 409–414.
5 A. R. Lippert, E. J. New and C. J. Chang, *J. Am. Chem. Soc.*, 2011, **133**, 10078–10080.
6 X. Li, X. Gao, W. Shi and H. Ma, *Chem. Rev.*, 2014, **114**, 590–659.
7 X. Chen, X. Tian, I. Shin and J. Yoon, *Chem. Soc. Rev.*, 2011, **40**, 4783–4804.
8 H. Kobayashi, M. Ogawa, R. Alford, P. L. Choyke and Y. Urano, *Chem. Rev.*, 2010, **110**, 2620–2640.
9 Y. Hong, J. W. Y. Lam and B. Z. Tang, *Chem. Soc. Rev.*, 2011, **40**, 5361–5388.
10 J. Li, L. Chen, L. Du and M. Li, *Chem. Soc. Rev.*, 2013, **42**, 662–676.
11 M. E. Roth, O. Green, S. Gnaim and D. Shabat, *Chem. Rev.*, 2016, **116**, 1309–1352.
12 T. Terai, E. Maki, S. Sugiyama, Y. Takahashi, H. Matsumura, Y. Mori and T. Nagano, *Chem. Biol.*, 2011, **18**, 1261–1272.
13 T. Peng, X. Chen, L. Gao, T. Zhang, W. Wang, J. Shen and D. Yang, *Chem. Sci.*, 2016, **7**, 5407–5413.
14 J. J. Hu, N.-K. Wong, M.-Y. Lu, X. Chen, S. Ye, A. Q. Zhao, P. Gao, R. Yi-Tsun Kao, J. Shen and D. Yang, *Chem. Sci.*, 2016, **7**, 2094–2099.

15 W. Chen, C. Liu, B. Peng, Y. Zhao, A. Pacheco and M. Xian, *Chem. Sci.*, 2013, **4**, 2892–2896.
16 J. Chan, S. C. Dodani and C. J. Chang, *Nat. Chem.*, 2012, **4**, 973–984.
17 H. Ischiropoulos, L. Zhu and J. S. Beckman, *Arch. Biochem. Biophys.*, 1992, **298**, 446–451.
18 K. A. Broniowska, C. E. Mathews and J. A. Corbett, *J. Biol. Chem.*, 2013, **288**, 36567–36578.
19 F. C. Fang, *Nat. Rev. Microbiol.*, 2004, **2**, 820–832.
20 J. S. Stamler, S. Lamas and F. C. Fang, *Cell*, 2001, **106**, 675–683.
21 A. Sikora, J. Zielonka, M. Lopez, J. Joseph and B. Kalyanaraman, *Free Radical Biol. Med.*, 2009, **47**, 1401–1407.
22 X. Sun, Q. Xu, G. Kim, S. E. Flower, J. P. Lowe, J. Yoon, J. S. Fossey, X. Qian, S. D. Bull and T. D. James, *Chem. Sci.*, 2014, **5**, 3368–3373.
23 N. A. Sieracki, B. N. Gantner, M. Mao, J. H. Horner, R. D. Ye, A. B. Malik, M. E. Newcomb and M. G. Bonini, *Free Radical Biol. Med.*, 2013, **61**, 40–50.
24 T. Peng, N.-K. Wong, X. Chen, Y.-K. Chan, D. H.-H. Ho, Z. Sun, J. J. Hu, J. Shen, H. El-Nezami and D. Yang, *J. Am. Chem. Soc.*, 2014, **136**, 11728–11734.
25 X. Li, R.-R. Tao, L.-J. Hong, J. Cheng, Q. Jiang, Y.-M. Lu, M.-H. Liao, W.-F. Ye, N.-N. Lu, F. Han, Y.-Z. Hu and Y.-H. Hu, *J. Am. Chem. Soc.*, 2015, **137**, 12296–12303.
26 E. W. Miller, A. E. Albers, A. Pralle, E. Y. Isacoff and C. J. Chang, *J. Am. Chem. Soc.*, 2005, **127**, 16652–16659.
27 A. R. Lippert, G. C. Van de Bittner and C. J. Chang, *Acc. Chem. Res.*, 2011, **44**, 793–804.
28 K. Kim, H. Yang, S. Jon, E. Kim and J. Kwak, *J. Am. Chem. Soc.*, 2004, **126**, 15368–15369.
29 S. A. Sundberg, R. W. Barrett, M. Pirrung, A. L. Lu, B. Kiangsoontra and C. P. Holmes, *J. Am. Chem. Soc.*, 1995, **117**, 12050–12057.
30 M. Hengsakul and A. E. Cass, *Bioconjugate Chem.*, 1996, **7**, 249–254.
31 T.-W. Wu, F.-H. Lee, R.-C. Gao, C. Y. Chew and K.-T. Tan, *Anal. Chem.*, 2016, **88**, 7873–7877.
32 R. Hu, J. Feng, D. Hu, S. Wang, S. Li, Y. Li and G. Yang, *Angew. Chem., Int. Ed.*, 2010, **49**, 4915–4918.
33 M. Taki, S. Iyoshi, A. Ojida, I. Hamachi and Y. Yamamoto, *J. Am. Chem. Soc.*, 2010, **132**, 5938–5939.
34 R. J. Singh, N. Hogg, J. Joseph, E. Konorev and B. Kalyanaraman, *Arch. Biochem. Biophys.*, 1999, **361**, 331–339.
35 J. L. Trackey, T. F. Uliasz and S. J. Hewett, *J. Neurochem.*, 2001, **79**, 445–455.
36 M. Kirsch and H. de Groot, *J. Biol. Chem.*, 1999, **274**, 24664–24670.
37 F. J. Martin-Romero, Y. Gutiérrez-Martin, F. Henao and C. Gutiérrez-Merino, *J. Fluoresc.*, 2004, **14**, 17–23.
38 P. Pacher, J. S. Beckman and L. Liaudet, *Physiol. Rev.*, 2007, **87**, 315–424.
39 A. G. McBride and G. C. Brown, *FEBS Lett.*, 1997, **417**, 231–234.
40 G. Ferrer-Sueta and R. Radi, *ACS Chem. Biol.*, 2009, **4**, 161–177.
41 S. Pfeiffer, E. Leopold, K. Schmidt, F. Brunner and B. Mayer, *Br. J. Pharmacol.*, 1996, **118**, 1433–1440.
42 J. M. Simons, B. A. Hart, T. R. Ip Vai Ching, H. Van Dijk and R. P. Labadie, *Free Radical Biol. Med.*, 1990, **8**, 251–258.
43 S. Heumuller, S. Wind, E. Barbosa-Sicard, H. H. Schmidt, R. Busse, K. Schroder and R. P. Brandes, *Hypertension*, 2008, **51**, 211–217.
44 G. L. Squadrito, R. Cueto, A. E. Splenser, A. Valavanidis, H. Zhang, R. M. Uppu and W. A. Pryor, *Arch. Biochem. Biophys.*, 2000, **376**, 333–337.
45 M. C. Krishna, A. Russo, J. B. Mitchell, S. Goldstein, H. Dafni and A. Samuni, *J. Biol. Chem.*, 1996, **271**, 26026–26031.
46 M. K. Stern, M. P. Jensen and K. Kramer, *J. Am. Chem. Soc.*, 1996, **118**, 8735–8736.
47 J. Zielonka, A. Sikora, J. Joseph and B. Kalyanaraman, *J. Biol. Chem.*, 2010, **285**, 14210–14216.
48 J. A. Fee and C. Bull, *J. Biol. Chem.*, 1986, **261**, 13000–13005.
49 C. Amatore, S. Arbault and A. C. W. Koh, *Anal. Chem.*, 2010, **82**, 1411–1419.
50 M. K. Hulvey, C. N. Frankenfeld and S. M. Lunte, *Anal. Chem.*, 2010, **82**, 1608–1611.
51 A. Kumar, S. H. Chen, M. B. Kadiiska, J. S. Hong, J. Zielonka, B. Kalyanaraman and R. P. Mason, *Free Radical Biol. Med.*, 2014, **73**, 51–59.